- ORIGINAL ARTICLE -

Heuristic Method for Photo-detectors Localization over Continuous Crystal Scintillation Cameras

Ramiro G. Rodríguez Colmeiro[1,2] and Claudio A. Verrastro[1,2]

[1] *GIAR, Universidad Tecnológica Nacional, Buenos Aires, Argentina*
Rodriguez.Colmeiro@Gmail.com
[2] *Comisión Nacional de Energía Atómica, Buenos Aires, Argentina*
cverra@cae.cnea.gov.ar

Abstract

The construction process of large scintillation cameras with continuous crystals is a complex problem affected by multiple variables, from the physical construction of the scintillation crystal to the dispersion in the sensibility of photomultiplier tubes. The selection of these variables have a strong impact on the final performance of the scintillation camera. A new method to select photomultiplier is presented in this paper, regarding its gain, making use of k-means clustering and genetic algorithms. The proposed algorithm was tested and applied in the construction of six scintillation cameras for the Argentinean positron emission tomogaph prototype (AR-PET), a problem with more than 10^{+600} possible configurations. The resulting configuration of the scintillation cameras reduced the software-free-calibration *FWHM* of the camera from 20% to 15% average.

Keywords: Anger Camera, Genetic algorithms, PET tomography, Photomultiplier placement, Scintillation cameras

1 Introduction

The construction of large scintillation cameras with continuous crystals is a complex problem and the effects of a wrong configuration directly affect the final resolution of the camera. This problem becomes even more complex when the number of photomultiplier tubes (PMT) to be used is large. In the AR-PET prototype[1], as well as in other devices, the scintillation cameras are formed by a large continuous NaI(Ti) crystal [2] populated with PMT, which are placed according to figure 1 covering the whole crystal surface. The interaction of a gamma ray with the scintillating material result in to the production of hundreds or thousands of luminous photons, its number depends on the efficiency of the scintillator material and the energy of the incident gamma ray. These light photons generate an omnidirectional flash, that is, some of the photons are reflected on the opposite side and at the edges of the scintillating crystal. Therefore the PMTs near the edge of the crystal receive significantly more light than those of the center. Also, the PMT tubes have a high gain dispersion from unit to unit given the same electrical operation conditions, which derives from its fabrication process [3] and the control of its gain is limited.

To achieve a uniform event rate for the whole surface of the scintillation crystal it is necessary to equalize the energy gain and quantum efficiency of each PMT. In addition, for PET application, it is necessary to equalize the transit time of each PMT, the transit time is modified when changing the high voltage between anode and cathode[3] and therefore is fixed at the same value for all the PMTs in the camera. Because of this to equalize the gain of the PMTs it is preferred to control the voltage between two dinodes of the PMTs[4].

There exist several approaches to reduce the effect of the photomultiplier gain dispersion, the most common is using software coefficients and count skimming[5] or performing single-PMT calibration using its spectral information[6]. Hardware methods have also been studied like *PMT-quadrant-sharing* techniques[7] and also including LED's inside the scintillation camera to calibrate PMTs by groups[8] or directly calculating correction matrices at hardware level[9]. The reduction of photomultiplier groups by segmenting the crystal is also common design choice which reduces this problem[10] but not applicable to continuous crystals.
All of the cited methods are focused on the correction of the PMT gain after it is placed inside the scintillation camera, taking for a fact that every unit

Citation: R. G. Rodríguez Colmeiro and C. A. Verrastro. *Heuristic Method for Photo-detectors Localization over Continuous Crystal Scintillation Cameras*. Journal of Computer Science & Technology, vol. 18, no. 1, pp. 12-17, 2018.
DOI: 10.24215/16666038.18.e02
Received: August 22, 2017 **Revised:** November 30, 2017 **Accepted:** December 08, 2017.
Copyright: This article is distributed under the terms of the Creative Commons License CC-BY-NC.

can be placed to work at every location inside the scintillation crystal. While this might hold if one is able to choose from a large set of PMT units and can, therefore, choose those of similar characteristics, in the case where the amount of PMT units to be placed is not large enough to disregard the large PMT gain variation some PMT localization intelligence must be applied. As far as the authors know, there is no report on PMT localization algorithms that study this particular subject.

In order to create working scintillation cameras with few slack PMT units while improving the initial acquisition efficiency, a new method was developed which automatically generate sub-optimal PMT configuration for each scintillation camera using k-nearest neighbor clustering and genetic algorithms to explore the possible configurations.

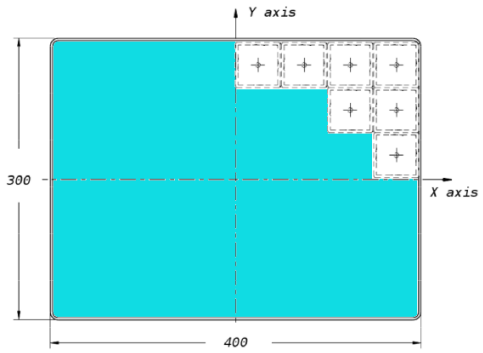

Figure 1: Photomultiplier tube disposition (white) on scintillation crystal (colored background). (Image courtesy of E. Venialgo, 2011 IEEE N.S.S.)

2 Problem Modelling

The definition of an adequate configuration of PMT in the scintillation camera requires knowing the behavior of both the scintillation crystal edges and the PMT dinode modulation.

It was developed a model to calculate the optimality of a configuration without using more powerful tools, such as GATE[11] that requires high computation times.

2.1 Crystal Reflection

The first effect is a consequence of the construction of the crystal, which is covered with a refractive paint in order to direct all scintillation photons to the crystal surface, the structure of the camera which holds the PMTs and the optic coupling of the PMTs with the crystal. The refractive paint is important to avoid losing light o over the edges of the crystal and enables the chamber to measure the deposited energy of the gamma ray. As a counter-effect the PMT placed in the edge receives more light if a gamma ray hits below this PMT center than the amount it would receive if the same ray hits below the PMT when it is placed in the center of the crystal.

Using the simulation software GATE a scintillation camera was modeled, following the AR-PET design and using ideal PMT units (perfect photon counting). A uniform gamma flat source was placed in front of the camera. The scintillation effect and visible photon transportation was simulated, obtaining the number of photons received by each PMT in every location of the crystal. Using the simulation results two factors were derived. These factors relate the energy observed when detecting an event in the corner or edge of the camera to detecting the same event at the center of the camera. Factors R_{C-C} and R_{C-E} of equations 1 and 2 represent the relation in photon count for the *center to corner* and *center to edge* respectively.

$$\mathrm{R}_{C-C} = \frac{\sum_{n_{Pos}=1}^{Num_{Pos}} \mathrm{Photons}_{Corner}}{\sum_{n_{Pos}=1}^{Num_{Pos}} \mathrm{Photons}_{Center}} = 1.52 \qquad (1)$$

$$\mathrm{R}_{C-E} = \frac{\sum_{n_{Pos}=1}^{Num_{Pos}} \mathrm{Photons}_{Edge}}{\sum_{n_{Pos}=1}^{Num_{Pos}} \mathrm{Photons}_{Center}} = 1.21 \qquad (2)$$

2.2 Photomultiplier Gain

The non-linearity and high gain dispersion between different PMTs for the same high voltage (HV) and dinode values make them difficult to characterize.

To test this behavior a custom calibration procedure is used. In the calibration process, the PMT is coupled with a $1'$ thick, $3'$ diameter NaI(tl) crystal from Saint-Gobain^{TM}[12] and placed within a dark chamber. The detector set is then exited with a Cs-137 source and the peak ADC channel for each pre-defined working points. For each PMT four distinct anode-cathode HV values and five dinode voltages where tested, making 20 different working points. The measured working points can be represented by four curves as shown figure 2. The observed behavior was fitted using a sigmoid curve, it reflects the non-linearity, both at the beginning, when the dinode is short-circuited and when it saturates.

Since this curves are generated using a calibration procedure and not the actual scintillation cameras, a correspondence factor (F_x) between the calibration crystal and camera was also derived. This factor was calculated by testing a group of PMTs in each possible position of the scintillation camera and then calibrated. Since the assembly of a scintillation camera is a complex process, only one group of 48 PMTs where tested. The obtained factor relates the amount of light received during the calibration and the different positions within the camera. The factor is calculated as the ratio between the ADC channel during calibration

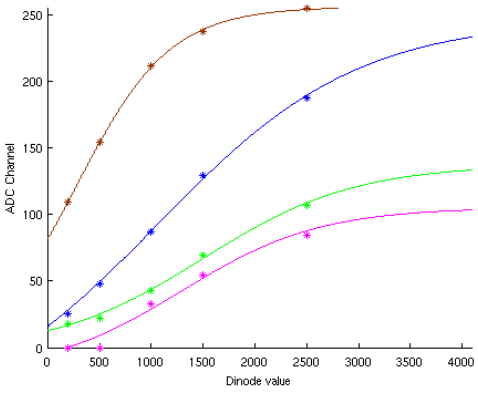

Figure 2: Photomultiplier tube working points and the aproximated curve. HV values: 1300 v (top curve), 1200 v (second to top), 1100 v (second to bottom) and 1000 v (bottom).

and ADC channel within the camera, as showed in eq. 3. One factor per position group was derived. The resulting factors where: $F_{Center} = 0.44$, $F_{Edge} = 0.54$ and $F_{Corner} = 0.71$.

$$F_x = \frac{ADC_{Characterization}}{ADC_{Scint.Camera}} \tag{3}$$

3 K-means pre-processing

The starting point of the configuration algorithm is the preprocessing of the problem using k-means clustering. The possible starting configurations are given by the amount of PMT units available and the amount of PMT to be placed in the different scintillation cameras to be constructed, this respond to the permutation formula (4), where n is the number of PMT units and k the units to be placed.

$$P = \frac{n!}{(n-k)!} \tag{4}$$

In order to generate a good starting point, which help the convergence of the later genetic algorithm, the PMTs are clustered around common HV. The Clusters are created by choosing a target ADC channel for the peak energy and measuring the similarity of the dinode values. By making use of the k-means algorithm [13] 3 clusters of PMTs are generated for each HV value. Each of the 3 cluster centers is in units of dinode value and their value is not given a-priori, the algorithm converges to them by using the target ADC channel and the F_{Center}, F_{Edge} and F_{Corner} factors, that means, one cluster per position in the scintillation camera. From this groups, the elements nearer to the cluster center are extracted, for a given HV, which holds the lower dispersion of dinode values. If multiple cameras are to be generated, the PMTs for the first camera are extracted from the list and the selection process is repeated until all cameras are populated.

4 Genetic Algorithm

Since an exhaustive exploration of the problem is not possible a sub-optimal search was proposed. The genetic algorithms are fit for this task and are proven to converge [14]. This technique requires the description of *individuals*, which in this case are feasible configurations of the scintillation cameras. The individual is described as the order of the PMTs inside the scintillation cameras to be constructed and the HV value of each of this cameras. The resulting *genome* of the individual is a vector of $[(k+1)*m]+L$ elements, where k is the amount of PMTs per camera and m is the number of cameras to be constructed and L is a slack variable, which represents the number of remaining PMTs which are selected as "spares" for the cameras. This slack PMTs will not be considered in the fitness calculation but are used in the mutation process.

At the beginning a population P of configurations is created using the K-means clustering, with more than $N = 30$ individuals. The starting fitness of the population is calculated using the process described in section 4.1 and then the selection process is applied. This selection process is done by mutation and elitism. In every iteration a given amount "$E > 0$" of parent individuals is selected to be copied unmodified to the next iteration of the algorithm, this is called *elitism*. Then a *mutation* process is applied to the population, as described in section 4.2, the *crossover* process is not used. The fitness value of each individual of the new population is computed and the probability S_n of each individual to survive is given by eq. 5. After the selection process, a new population P^{+1} is created and the algorithm proceeds to the next iteration. This is repeated until an individual full-fills the target criteria or the number of iterations is exhausted.

$$S_n = \frac{F_n}{\sum_{i=1}^{N} F_i} \tag{5}$$

4.1 Fitness calculation

The fitness reflects the dinode voltage difference between PMTs at the same HV. In this sense, the lower the fitness value the better is the configuration (individual).
The fitness of the configuration is calculated as the largest of the maximum difference of dinode values computed inside each scintillation camera. This measure is described by equations 6 and 7, where D are the dinode voltages of each PMT in the camera. This metric was chosen since the worst case is given when a PMT is limited by a low dinode voltage and other is limited by a high dinode voltage, this would limit the

fine-tuning possibilities of the dinode value after the selection process described by this work.

$$F_m = max(D) - min(D) \tag{6}$$

$$F_n = max(F_1, F_2, ..., F_m) \tag{7}$$

4.2 Mutation

The mutation process can occur in two different ways.

The first way is the most probable, with a probability below 10% for each of the scintillation cameras that compose the individual, if a camera is selected to be mutated one PMT of it is randomly selected, then, another camera of the same individual is selected randomly and a PMT from this camera is also randomly selected. This two selected PMTs are swapped and both cameras are reconfigured using all the PMTs which belong to their respective groups. If there are slack PMTs, they are considered in both processes, swapping and reconfiguration.

The second way mutation process is much less probable, and it changes the HV of the camera, the probability of this mutation is bellow 1%. If a camera is chosen, its HV is selected randomly to any calibrated value.

5 Results

This algorithm was tested for the configuration of the AR-PET prototype of CNEA[15]. The AR-PET has 6 scintillation cameras, each consisting of 48 PMTs. For the construction of this cameras a total of 307 PMT units where available. Using eq. 4 the total amount of possible configurations where calculated and it surpasses 6 10^{+605}.

5.1 Scintillation camera characterization

The first step of the process was the characterization of the scintillation camera using a pre-configured scintillation camera, as described at the end of section 2.2. The calibration process was done using a Cs-137 source. Knowing the calibration points of each PMT the relationships between each group (Center, Edge and Corner) where calculated. In figure 3 the simulation results and empirical testing are compared, it can be seen that the obtained values agree. This is also seen in equations 8 and 9, where the agreement to the values calculated in eq. 1 and eq. 2 is more than the 94% in the worst case.

$$R_{C-C}^{Empirical} = \frac{F_{Corner}}{F_{Center}} = 1.61 \tag{8}$$

$$R_{C-E}^{Empirical} = \frac{F_{Edge}}{F_{Center}} = 1.22 \tag{9}$$

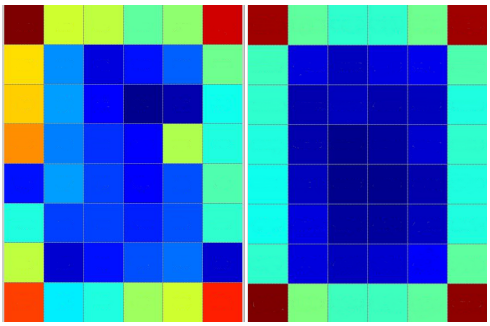

Figure 3: Ratio of the expected amount of light received in the center of the camera to the light received in each PMT. The picture on the left shows the empirical measure while the picture on the right shows the GATE simulation results.

5.2 Configuration comparison

The existing prototype scintillation camera was created by hand-picking each PMT from the total 307 PMT, assigning those with less gain to the corners, where they received more light, those with more gain to the edges and finally, the ones with the most gain to the center. This process was done without any reservation in order to build the other 5 cameras, since it was a prototype. The chosen objective ADC channel for the peak energy of the Ce-137 was channel 100 of 255. The HV tension was chosen to be 1200 V. The resulting scintillation camera has a fitness value of 1521, as was calculated by eq. 6. In figure 4 the interpolated curves of each PMT for the chosen HV composing camera are drawn, this curves are affected by the gain factors modelled in 5.1.

The AR-PET cameras were calculated using the process described in this work, using a population of 12 individuals, an elitism value of 10%, probability of mutation of 6% for the first type and 0.6% for the second type and 1000 iterations. No ending criteria were used. The resulting fitness values of the resulting 6 cameras are summarised, along with the prototype camera, in table 1. In figure 5 the PMT curves of the camera with the worst fitness value, which define the fitness of the individual, is shown to serve as a comparison with the prototype camera (figure 4).

Table 1: Scintillation cameras fitness values

Camera	HV [v]	Fitness
1	1200	759
2	1100	771
3	1100	741
4	1300	773
5	1200	757
6	1200	684
Prototype	1200	1521

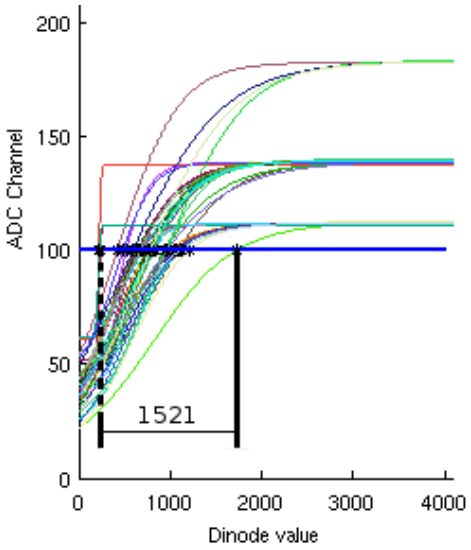

Figure 4: PMT curves of the prototype scintillation camera. PMTs where hand-picked. The thick horizontal line represents the target ADC peak, the black dot in the intersection of each curve with the line indicates the working point of the PMT. The dimension represents the fitness value.

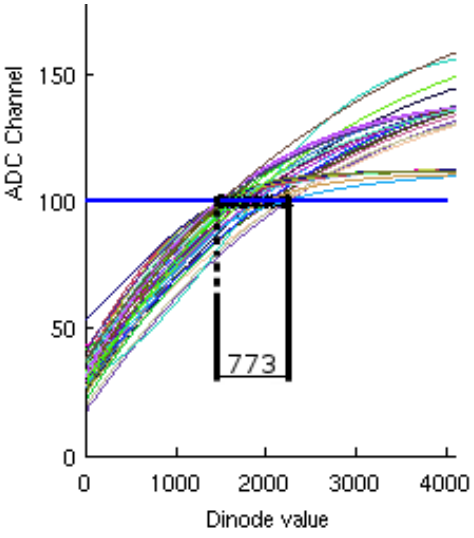

Figure 5: PMT curves corresponding to camera number 4, which presents the configuration with the highest fitness value (lowest performance) among 6 cameras assembled using this method. The horizontal blue line represents the target ADC peak, the intersection of each curve with the blue line marks the working point of each PMT.

6 Conclusion

This work proved to be able to model the light distribution within the scintillation camera and correlate the parametrization of the PMTs working points with their final placement within the camera. This enables to automatize the measuring process and makes it independent of the final placement of the PMT unit.

The k-means clustering along with the genetic algorithm proved to reduce the dispersion of dinode values within the scintillation camera significantly, it also was able to found out a viable configuration for all the requested cameras with a slack amount of PMT of less than the 7% of the total available units. The cameras constructed with this method achieve an FW-HM (Full-width Half-Maximum) of 15% without fine-tuning, improving previous results[16]. Another advantage is that assembled cameras have working points near the lineal dinode voltage vs gain zones of the PMTs.

Acknowledgement

The authors would like to thank Ing. Hernández Estevenz Ariel, Ing. Scremin Matías Ariel, Msc. Federico De La Cruz Arbizu and Pirlo Damián Ezequiel, of the National Nuclear Energy Commission (CNEA) for their support with the measurements and equipment assembly.

Competing interests

The authors have declared that no competing interests exist.

References

[1] C. Verrastro, M. Belzunce, J. C. Gomez, D. Estryk, E. Venialgo, F. Carmona, and D. De Biase, "De la primera radiografía al primer tomógrafo por emisión de positrones argentino," *Proyecciones*, p. 49, 2009.

[2] Saint-Gobain Ceramics & Plastics, "Nai(tl) and polyscin nai(tl) sodium iodide," 2005.

[3] HAMAMATSU PHOTONICS K.K, "Photomultiplier tubes," 2007.

[4] Y. Liu, H. Li, Y. Wang, T. Xing, S. Xie, J. Uribe, H. Baghaei, R. Ramirez, S. Kim, and W.-H. Wong, "A gain-programmable transit-time-stable and temperature-stable pmt voltage divider," in *Nuclear Science Symposium Conference Record, 2003 IEEE*, vol. 5, pp. 3101–3104, IEEE, 2003.

[5] G. Knoll and M. Schrader, "Computer correction of camera nonidealities in gamma ray imaging," *IEEE Transactions on Nuclear Science*, vol. 29, no. 4, pp. 1271–1279, 1982.

[6] Y. Wang, W.-H. Wong, M. Aykac, J. Uribe, H. Li, H. Baghaei, Y. Liu, and T. Xing, "An iterative energy-centroid method for recalibration of pmt

gain in pet or gamma camera," in *Nuclear Science Symposium Conference Record, 2001 IEEE*, vol. 4, pp. 1965–1968, IEEE, 2001.

[7] H. Li, W.-H. Wong, Y. Wang, Y. Liu, T. Xing, J. Uribe, H. Baghaei, and R. Farrell, "Front-end electronics based on high-yield-pileup-event-recovery method for a high resolution pet camera with pmt-quadrant-sharing detector modules," in *Nuclear Science Symposium Conference Record, 2002 IEEE*, vol. 2, pp. 699–703, IEEE, 2002.

[8] H. Li, Y. Liu, T. Xing, Y. Wang, J. Uribe, H. Baghaei, S. Xie, S. Kim, R. Ramirez, and W.-H. Wong, "An instantaneous photomultiplier gain calibration method for pet or gamma camera detectors using an led network," in *Nuclear Science Symposium Conference Record, 2003 IEEE*, vol. 4, pp. 2447–2451, IEEE, 2003.

[9] E. Stoub, "Method and circuit for stabilizing conversion gain of radiation detectors of a radiation detection system," Apr. 15 1986. US Patent 4,583,187.

[10] T. E. Peterson and L. R. Furenlid, "Spect detectors: the anger camera and beyond," *Physics in medicine and biology*, vol. 56, no. 17, p. R145, 2011.

[11] "Gate." Available at: `http://www.opengatecollaboration.org`. Accessed on 2017-02-14.

[12] "http:www.detectors.saint-gobain.com." Accesed on 2017-11-23.

[13] S. Lloyd, "Least squares quantization in pcm," *IEEE transactions on information theory*, vol. 28, no. 2, pp. 129–137, 1982.

[14] R. O. Duda, P. E. Hart, and D. G. Stork, *Pattern Classification (2Nd Edition)*. Wiley-Interscience, 2000.

[15] C. A. Verrastro, M. L. Cabrejas, D. Estryk, E. Venialgo, S. Marinsek, M. Belzunce, J. Zalcman, L. M. Giuliodori, R. Barneda, F. Carmona, D. D. Biase, M. Dalletesse, S. Villalba, C. Pulitze, F. Dufort, A. Cervantes, and J. Camenforte, "Ar-pet: Primer tomógrafo por emisión de positrones argentino," in *IXXXV Reunión Anual de la Asociación Argentina de Tecnología Nuclear (AATN)*, 2008.

[16] E. Venialgo, C. Verrastro, D. Estryk, and M. Belzunce, "Método de calibración para cámara gamma y pet con una medición única de campo inundado," *XIII reunión de Trabajo en Procesamiento de la Información y Control*, pp. 1010–1015, 2009.